JOURNAL OF Applied Polymer SCIENCE

Controlled Degradation of Polylactic Acid Grafting *N*-Vinyl Pyrrolidone Induced by Gamma Ray Radiation

Chaorong Peng,[1] Hao Chen,[1] Jingxia Wang,[1] Zhuping Chen,[1] Maojun Ni,[1] Yuheng Chen,[1] Jing Zhang,[1] Tun Yuan[2]

[1]Radiation Chemistry Department, Sichuan Institute of Atomic Energy, Chengdu 610101, People's Republic of China
[2]Engineering Research Center in Biomaterials, Sichuan University, Chengdu 610064, People's Republic of China
Correspondence to: H. Chen (chenghao_siae@163.com)

ABSTRACT: Polylactic acid (PLA) films were surface modified by gamma ray irradiation-induced grafting of *N*-vinyl pyrrolidone (NVP). The *in vitro* degradation behavior of polylactic acid grafting *N*-vinyl pyrrolidone (PLA-*g*-PVP) copolymer was analyzed in terms of weight loss, molecular weight, and thermal properties. Grafting NVP significantly accelerated the degradation of PLA. The mass losses of the copolymers, which were less than that of pure PLA at the beginning of the degradation period, sharply accelerated with increasing degradation time. Moreover, the crystallization temperature decreased with increasing degradation time in the same graft ratio, and the degree of crystallinity increased. Cytotoxicity experiments and animal experiments *in vivo* were carried out to evaluate the biocompatibility of PLA-*g*-PVP copolymer. Varying graft ratios of PVP could control the degradation rate of copolymers, and thus broadening the applications of this material, such as in tissue engineering scaffolds, drug delivery, and prevention of post-surgical adhesion. © 2013 Wiley Periodicals, Inc. J. Appl. Polym. Sci. 130: 704–709, 2013

KEYWORDS: biodegradable; biocompatibility; grafting; irradiation; degradation

Received 1 November 2012; accepted 3 March 2013; published online 30 April 2013
DOI: 10.1002/app.39243

INTRODUCTION

Polylactic acid (PLA) is well known as a bioabsorbable material for many applications such as sutures, pins, screws, and drug delivery systems.[1–3] However, PLA may not completely meet the requirements for several applications because of its poor hydrophilicity, and low degradation rate.[4] These disadvantages are overcome by different methods, such as blending with hydroxyapatite or calcium phosphate and polyvinyl alcohol,[5–7] chemical synthesis of the block copolymer,[8,9] ultraviolet irradiation modification,[10,11] and gas plasma modification.[12] Gamma ray irradiation-induced grafting has superior advantages, including simplicity, low cost, controllable process, and adjustable material composition and structure. This method assures the grafting of monomers that are difficult to polymerize by conventional methods without initiator and catalyst residues.[13] Poly(*N*-vinyl pyrrolidone) (PVP) is a nontoxic polymer with excellent biocompatibility and water solubility; it has been applied in various medical fields.[14–16] Our previous study indicates that a predictable graft ratio can be obtained by controlling the radiation dose and graft conditions.[17] Therefore, preparing PLA-*g*-PVP copolymers with different graft ratios in a wider range is feasible.

PLA degradation is a complex process that has been extensively investigated.[18,19] The mechanisms of polymer degradation are affected by many variables such as chemical structure, crystallinity, molecular weight, processing conditions, shape, and size. In this study, PLA-*g*-PVP copolymers with different graft ratios were prepared, and the *in vitro*-controlled degradation behaviors and biocompatibilities of the copolymers were investigated.

MATERIALS AND METHODS

Materials

PLA (avg., $M_\eta = 4.0 \times 10^5$) was obtained from Chengdu Dikang Biomedical Material (Chengdu, China). NVP obtained from Sigma-Aldrich (USA) was purified through vacuum distillation before use. Chloroform, ethyl alcohol, and methanol were obtained from Kelong Agent (Chengdu, China).

PLA Grafting and Characterization

PLA films were cast from a 1.6 wt % chloroform solution by solvent evaporation at room temperature, dried at 38°C in a vacuum, and then cut into small squares. PLA films and the grafting solution composed of monomer and solvent were placed into glass tubes and then purged with nitrogen for 5 min. The glass tubes were subsequently sealed and irradiated by ^{60}Co-γ source at room temperature with a dose of 0.5–2.0 kGy. The grafted films

were first washed with water and then underwent ultrasonic cleaning (50 W) for 10 min in ethanol, dipped in ethanol for 48 h at room temperature to remove residual monomer and homopolymer, and then dried to constant mass in vacuum at 38°C. The PLA-*g*-PVP copolymer with different graft ratios is denoted as PLA-*g*-PVP(*Y*%), where *Y*% represents the graft ratio.

Microstructure. The structures of PLA and PLA-*g*-PVP films were represented by attenuated total reflection Fourier transform infrared spectroscopy (ATR-FTIR) on a Thermo Fisher Nicolet IS 10 FTIR spectrometer with a wavelength ranging from 4000 to 500 cm^{-1}.

Graft Ratio. The graft ratio was calculated as follows:

$$\text{Graft ratio } (\%) == \frac{w_g - w_r}{w_r} \times 100\% \quad (1)$$

where w_r and w_g are the film weights before and after grafting, respectively.

Hydrophilic Property. The hydrophilic property of PLA-*g*-PVP was analyzed by surface contact angle and water absorption performance. The surface contact angle of PLA-*g*-PVP was determined using a contact angle instrument (KRUSS DAS30, Hamburg, Germany) and film samples with 25 mm^2 × 50 mm^2 dimensions and 0.1 mm thickness. Water absorption performance was determined by soaking the film in distilled water for 48 h, blotting the surface water, and then recording the swollen weight. Water absorption was calculated as follows:

$$\text{Water uptake } (\%) = \frac{w_2 - w_1}{w_1} \times 100\% \quad (2)$$

where w_1 and w_2 are the polymer weights before and after water absorption, respectively.

***In Vitro* Degradation**

The traditional promoting test according to ISO 10993-13:1998 was used to investigate the degradation within a short period. The copolymer films of different graft ratios and pure PLA were cut into squares (2 cm × 2 cm; 30–45 mg each) and separately immersed in phosphate-buffered saline (pH = 7.4, 70°C) for 6, 12, 24, 48, 72, 96, 120, 144, and 168 h. Subsequently, the films were washed with distilled water and ethanol before vacuum drying at 38°C for 48 h. The dry weights were recorded, and the samples were used for further analysis. The water uptake of pure PLA and copolymers during the degradation process was calculated as Formula 2.

Mass Loss. Mass loss was calculated as follows:

$$\text{Mass loss } (\%) = \frac{w_t - w_0}{w_0} \times 100\% \quad (3)$$

where w_0 is the initial weight of the specimen and w_t is the weight of the dried specimen at time *t*.

Molecular Weight. The molecular weight was tested using the Ubbelohde viscometer method:

$$[\eta] = KM^{\alpha} \quad (4)$$

where $[\eta]$ and M represent the intrinsic viscosity and molecular weight, respectively, with the values of the Mark–Houwink constants for PLA, $K = 5.45 \times 10^{-3}$ mL/g and $\alpha = 0.73$.

Differential Scanning Calorimetry. The differential scanning calorimetry (DSC) curves were recorded using a Netzsch DSC200F3 differential scanning calorimeter heated from 0 to 210°C at a rate of 20°C/min using nitrogen as purge gas. The crystallinity percentage (X_c) was calculated using the reference heat of enthalpy (93.1 J/g) for a theoretically 100% crystalline PLA.[20] In the case of the PLA-*g*-PVP copolymers, the heat of fusion (ΔH_f) and the heat of crystallization (ΔH_c) of the samples were recalculated according to the different degradation times.

Cell Toxicity and Implantation Response

3-(4,5-Dimethylthiazol-2-yl)-2,5-diphenyltetrazolium bromide Assay for Cytotoxicity Test. Mouse fibroblast cells (FCs) (ATCC CCL1, NCTC Clone 929, and Clone of Strain L) were proliferated at 37°C with 5% CO_2 in Petri dishes (Φ = 100 mm) containing RPMI 1640 (GIBCO BRL) supplemented with 10% fetal bovine serum and antibiotics (100 U/mL penicillin and 100 μg/mL streptomycin). After growing nearly confluent, the cells were trypsinized, collected, and then adjusted to 1 × 10^5 cells/mL for the succeeding experiments. Cytotoxicity was evaluated through the 3-(4,5-dimethylthiazol-2-yl)-2,5-diphenyltetrazolium bromide assay using well-grown passage L929 mouse fibroblasts under the standard ISO 10993.5-2009.

***In Vivo* Implantation.** Sixteen healthy Sprague–Dawley rats weighing 214–313 g were obtained from the breeding farm of the Sichuan Province Experimental Animal Special Committee. The PLA and PLA-*g*-PVP (graft ratio, 66%) samples were cut into small wafers (diameter, 0.8 mm; thickness, 0.1–0.13 mm), immersed in 75% alcohol for 4 h, and then placed into a glass bottle sealed and sterilized by γ-rays at 12 kGy. The molecular weights of the sterilized samples are 6.5 × 10^4 (pure PLA) and 7.5 × 10^4 (PLA-*g*-PVP).

The animals were prepared for conventional operation. The operational area was sterilized after anesthesia administration of pentobarbital sodium by peritoneal injection. The test and control articles were subcutaneously injected (0.5 mL per site) under the animal dorsal skin. Then, 20,000 U/kg gentamicin was injected once into the intramuscular. All animals were placed in intensive care until the implanting terminals were attained. At each end of the experimental periods (4, 12, 20, and 28 weeks), the animals were sacrificed with an overdose of pentobarbital sodium. The implants and surrounding tissues were retrieved for macroscopic and histopathological evaluation. The tissue blocks around the implants were fixed by 20% formalin. After the gradient ethanol was dehydrated, the samples were paraffin-embedded, sectioned, and then stained with hematoxylin and eosin (HE).

RESULTS AND DISCUSSION

PLA Grafting

Microstructures. Figure 1 shows the ATR spectra of pure PLA and PLA-*g*-PVP with different graft ratios. In the PLA spectrum [Figure 1(a)], the peaks can be observed at 1743, 1081, and 1453 cm^{-1} corresponding to the —C=O stretching, —C—O— stretching, and —CH_3 bending vibrations, respectively. The dramatic change in peaks [Figure 1(b–e)] at 1659–1667 cm^{-1} and at 1421 cm^{-1} because of the stretching mode of C=O and the methylene wagging mode of the pyrrolidone ring, respectively, were also observed. The signal intensity of the absorption bands centered at 1660 cm^{-1} was assigned to the —C=O stretching

Applied Polymer SCIENCE

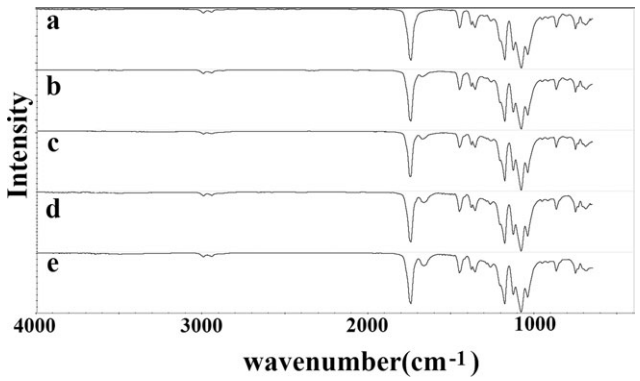

Figure 1. ATR spectra of PLA (a) and PLA-*g*-PVP with different graft ratios (b: 3.1%, c: 7.0%, d: 11.8%, e: 16.4%).

vibration of the pyrrolidone ring, which increased with increasing graft ratio.[17] Moreover, the spectra of PLA-*g*-PVP [Figure 1(b–e)] did not show the characteristic peaks of NVP at 1630 cm^{-1}, which demonstrated that the monomer and homopolymer of NVP were entirely removed.

Hydrophilic Property. The wettability of the PLA-*g*-PVP films was evaluated by measuring the surface contact angles and water absorption performance (Table I). The water contact angle of pure PLA was 82°, and those of the PLA-*g*-PVP copolymers slowly decreased to 74° as the grafting ratio increased from 3.1 to 16.4%. Water absorption increased from 0.4% for PLA to 5.7% for PLA-*g*-PVP (16.4%), indicating an enhanced wettability achieved by the grafting of hydrophilic PVP on the hydrophobic PLA surface.

In Vitro Degradation

Changes in Hydrophilic Property. The wettability of the PLA-*g*-PVP films was evaluated by measuring the water absorption performance during the degradation process (Figure 2). Grafting with different ratios of PVP resulted in a significantly greater hydrophilicity than that of pure PLA. Water absorption of pure PLA remained at 0.4–1.0% during the degradation process and did not show any significant increase. Water absorption of PLA-*g*-PVP (16.4%) was 5.7% at the beginning of degradation and increased to 12.8% at 168 h. The first step of the degradation is water uptake, followed by hydrolysis, which causes the breakage of the backbone ester bonds. The degradation of aliphatic polyesters is based on the hydrolytic reaction. When the water molecules attack the ester bonds in the polymer chains, the average length of the polymer chains becomes smaller. Eventually, the

Table I. Contact Angle and Water Absorption of PLA and PLA-*g*-PVP

	Contact angle (°)	Water absorption (%)
PLA	82	0.4
PLA-*g*-PVP (3.1%)	80	3.3
PLA-*g*-PVP (7.0%)	77	4.2
PLA-*g*-PVP (11.8%)	75	4.8
PLA-*g*-PVP (16.4%)	74	5.7

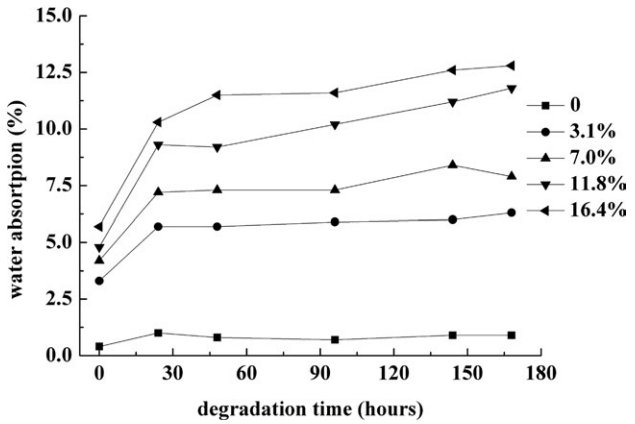

Figure 2. Water uptake of PLA and PLA-*g*-PVP with different graft ratios at different degradation times.

process produces short-chain fragments with carboxyl end-groups that are soluble in water.[21,22]

Mass Loss. Figure 3 shows the mass decline in the *in vitro* degradation of PLA and PLA-*g*-PVP with different graft ratios. The mass losses of pure PLA, PLA-*g*-PVP (3.1%), PLA-*g*-PVP (7.0%), PLA-*g*-PVP (11.8%), and PLA-*g*-PVP (16.4%) were 5.8, 1.5, 12.9, 22.5, and 37.8%, respectively, after 168 h of *in vitro* degradation. The mass loss increased with the increasing degradation time. In particular, the mass loss of PLA-*g*-PVP (16.4%) sharply increased after 36 h. The mass loss percentage seemed to depend on the PVP content, as the PVP branch caused the samples to become more hydrophilic and easier to degrade. The mass losses of the copolymers at the beginning of the degradation period were less than that of pure PLA. Acceleration with increasing degradation time was observed. The turning points of the copolymers with 16.4, 11.8, and 7.0% graft ratios occurred at 36, 72, and 96 h, respectively. The copolymer with 3.1% graft ratio indicated the least apparent mass loss, which was below 1.5% after 168 h. The lower mass loss of PLA-*g*-PVP compared with that of pure PLA was peculiar. This observation

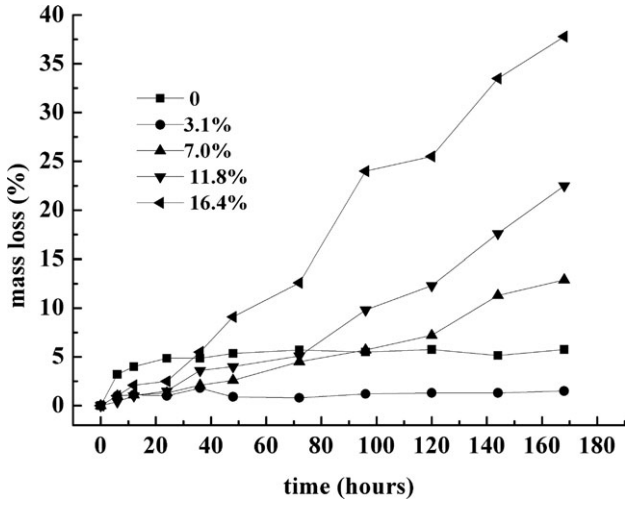

Figure 3. Mass losses in the *in vitro* degradation of PLA and of PLA-*g*-PVP with different graft ratios.

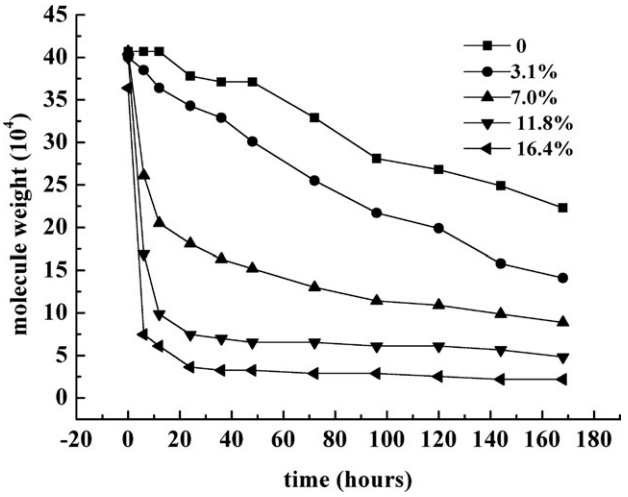

Figure 4. Molecular weight changes in the *in vitro* degradation of PLA-*g*-PVP with different graft ratios and PLA films.

may be owing to the crosslinking structures caused by low-dose irradiation, and thus preventing the degradation.[23] The gel content of the PLA-*g*-PVP was tested using chloroform as a solvent, but no obvious gel had been found. The microstructure of the PLA-*g*-PVP copolymer will be further investigated.

Molecular Weight. The *in vitro* hydrolytic degradation rate of PLA is dependent on molecular weight.[24] Figure 4 shows the molecular weight changes in the *in vitro* degradation of PLA and PLA-*g*-PVP with different graft ratios. Contrary to the gentle increase in mass loss in the initial degradation period, the molecular weight of the PLA-*g*-PVP dramatically decreased during the first 24 h when the grafting ratio was higher than 7.0%, and then the rate of decrease slowed down and leveled off. The degradation rate increased with the increasing content of PVP chains. The molecular weights of the copolymers with 7.0, 11.8, and 16.4% graft ratios decreased by 55.5, 81.4, and 90.0% after 24 h, and then by 78.2, 88.0, and 94.0% after 168 h, respectively. In comparison, the molecular weights of PLA-*g*-PVP (3.1%) and pure PLA gradually decreased by 14.3 and 7.1% after 24 h and then by 64.8 and 45.2% after 168 h, respectively. The tunable degradation rate can be attained by controlling the graft ratio of PVP. Moreover, the gamma ray irradiation may produce crosslink microstructures that prevent degradation in the early stage. Therefore, a biodegradable material that is relatively stable in the early period of degradation can be prepared and significantly degraded in the subsequent period of degradation.

Surface Compositions. Figure 5 shows the surface compositions of the PLA-*g*-PVP copolymers (16.4%) at different degradation times. The characteristic peaks responded to the relative PVP content in PLA. The area ratio of the characteristic peaks of PVP at 1667 cm^{-1} and of PLA at 1743 cm^{-1} decreased with the increasing degradation time. A new absorption band appeared at 1608 cm^{-1}, the intensity of which was relative to the degradation time. It initially appeared after 48 h and reached the highest intensity at 168 h. The new absorption band implies the decomposition and rearrangement of the

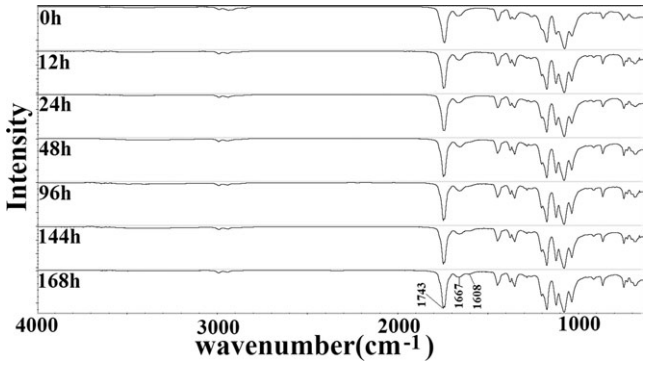

Figure 5. ATR spectra of the PLA-*g*-PVP copolymers (graft ratio, 16.4%) after different degradation times.

grafted PVP chains, as well as the formation of double bonds.[25,26] Moreover, the decrease in the characteristic peak of PVP at 1667 cm^{-1} also confirmed the breaking of grafted chains. However, even after longer degradation times, fractions of the grafted chains remain attached to the sample surface. This finding verifies that the functionalities are not lost upon 168 h of degradation.[27]

Changes in Thermal Behaviors. Figure 6 shows the DSC heating curves of PLA-*g*-PVP (3.1%) at different degradation times. The peak of heat enthalpy at 62°C reflects the glass transition of PLA. The second transition between 113 and 121°C is an exotherm peak, representing PLA-*g*-PVP cold crystallization. The third transition is endotherm at 178°C, caused by the melting of PLA in the copolymers. The degradation progressed from 6 to 168 h; the crystallization temperature gradually decreased from 121.1 to 113.4°C; and crystallinity increased from 33.7 to 43.3% (Table II). This observation is most likely attributed to the decrease in molecular weight and the increased molecular mobility of PLA chains with the increasing degradation time.

Biocompatibility

Cytotoxicity. For *in vitro* studies, FCs were seeded on tissue culture plastics, with lipopolysaccharide added to the culture medium of different leaching liquors. The FCs were cultured for

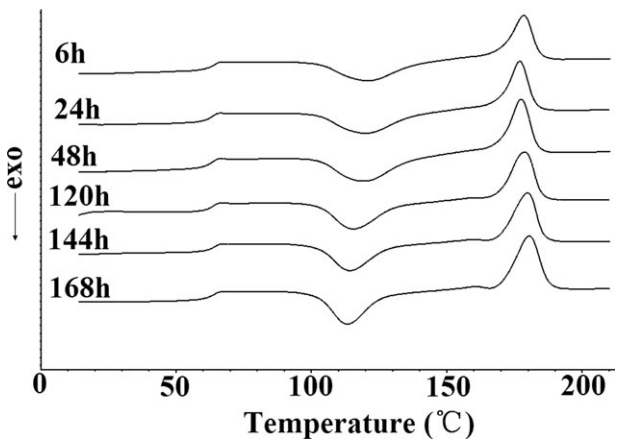

Figure 6. DSC curves of PLA-*g*-PVP (3.1%) after different degradation times.

Table II. Effect of Degradation Time on the Crystallinity of Copolymer with 3.1% Graft Ratio

Degradation time of copolymer (h)	$T_{c\ PLA}$ (°C)	$\Delta H_{c\ PLA}$ (°C)	$\Delta H_{m\ PLA}$ (°C)	X_m (%)
6	121.1	31.18	31.55	33.7
24	119.9	33.09	32.12	34.3
48	118.8	38.74	36.36	38.8
120	115.5	36.71	36.21	38.6
144	114.5	35.14	35.57	38.0
168	113.4	39.44	40.58	43.3

$T_{g\ PLA}$, melting temperature; $\Delta H_{c\ PLA}$, crystalline enthalpy; $\Delta H_{m\ PLA}$, melting enthalpy; $X_{m\ PLA}$, crystallinity.

24 h, during which the incubation effectively progressed in the PLA and PLA-*g*-PVP leaching liquors. After 24 h, the cell survival rates of PLA, and PLA-*g*-PVP leaching liquors concentrations of 25, 50, and 100% were 101.9, 109.5, 109.3, and 107.4%, respectively, and that of the positive control was 9.9%. Thus, we obtained grafted materials with higher cell survival rates. The cell survival rate of the PLA-*g*-PVP leaching liquor of different concentrations was slightly higher than that of PLA and the negative control (Table III). These results show that PLA-*g*-PVP has no cytotoxicity and is favorable for cell proliferation.

***In Vivo* Implantation Study.** All rats were effectively recovered after the operation. Throughout the implantation period, all animals showed no obvious systemic reaction. The wounds and surrounding skin healed after the operation. Both tissue response and degradation of materials *in vivo* could be observed. HE staining microscopic examination (Image 1) indicated that the copolymer films rapidly degraded, mainly beginning at 4 weeks (Image 1, T1). In contrast, the degradation of PLA films was slower, mainly appearing at 28 weeks as onion-shell materials (Image 1, C4). These results coincide with the previously discussed change in mass loss. Moreover, the interfaces of the PLA and copolymer films with the surrounding tissues were different. A large interspace appeared between the PLA films and the tissues (Image 1, C1–C4), which was caused by the poor hydrophilicity of the former. In contrast, the copolymer films exhibited excellent cell adhesion. The copolymer films and tissues were in close contact, and their interface was blurred (Image 1, T1–T4). At 12 weeks of implantation (Image 1, T2), the copolymer films began to infiltrate tissue for absorption. At 28 weeks of implantation (Image 1, T4), the copolymers films, which were decomposed by tissue cells, could not be distinguished from the tissues. PLA-*g*-PVP had a faster degradation rate and better cell affinity, enabled easier cell growth into the material to form new tissue. The copolymer films showed a slight inflammatory reaction to the surrounding tissue, which might be caused by the hydrolyzed lactic acid during the speedy degradation. The slight inflammatory reaction is acceptable to the requirements of ISO 10993-6:2007. In general, the slight inflammatory reaction is preferred in cases of rapid healing. For example, the inflammatory reaction stimulates and accelerates the regeneration of certain epithelial tissues.[28] The results of *in*

Table III. Cell Survival Rate for Different Concentrations of the PLA-*g*-PVP Leaching Liquor, PLA Leaching Liquor, Positive Control, and Negative Control

	Positive control	Negative control	PLA leaching liquor	25% Leaching liquor	50% Leaching liquor	100% Leaching liquor
Cell survival rate (%)	9.9	101.3	101.9	109.5	109.3	107.4

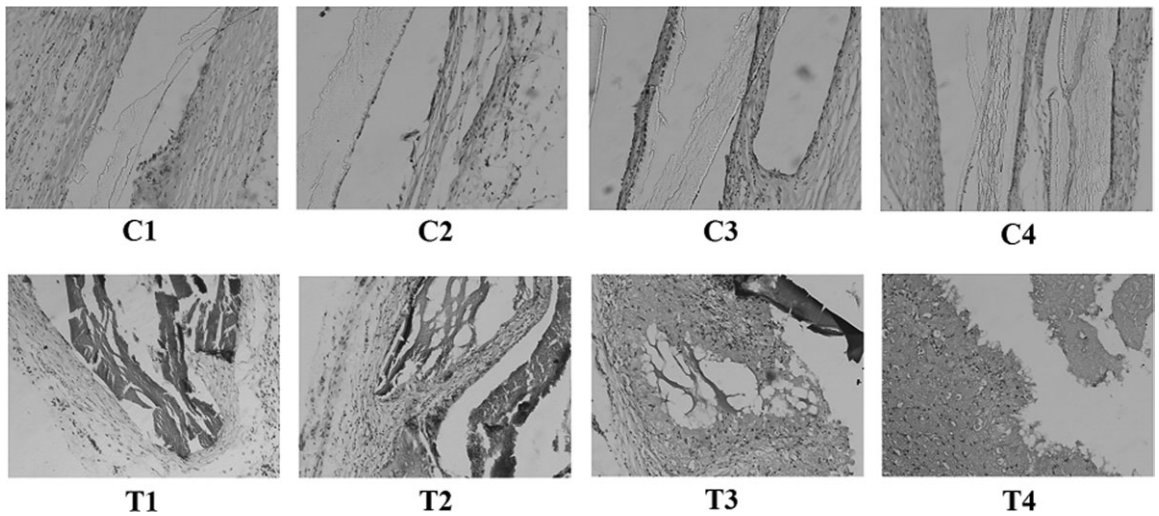

Illustration 1. Microscope observation of implanted wafers of PLA (C1–C4) and PLA-*g*-PVP (T1–T4) at 4, 12, 20, and 28 weeks (HE × 100).

vivo implantation study show that PLA-*g*-PVP copolymer has better cell affinity and faster degradation rate, making it seem like an ideal biomaterial for tissue repair.

CONCLUSIONS

This study focused on controlling the degradation and biocompatibility of PLA-*g*-PVP induced by gamma ray irradiation. Experiments on *in vitro* degradation reveal that the degradation rate and hydrophilicity of the copolymer were significantly affected by the PVP chains and could be finely tuned by different PVP graft ratios. The mass losses of the copolymers, which were less than that of pure PLA at the beginning of the degradation period, accelerated with increasing degradation time. The copolymers with higher PVP content attained better hydrophilicity, biocompatibility, and faster degradation rate in the later period of degradation. During the degradation process, the obvious mass losses of the copolymers with 16.4, 11.8, and 7.0% graft ratios occurred at 36, 72, and 96 h, respectively. ATR-FTIR and DSC tests indicate that the graft chains remain attached to the sample surface upon 168 h of degradation and that the copolymer crystallinity increased with the increasing degradation time. The results of cell toxicity and implantation response on PLA-*g*-PVP copolymer demonstrate that the copolymer has better biocompatibility than PLA. Therefore, grafting copolymers with controllable degradation rates show potential value in biomaterial applications.

ACKNOWLEDGMENTS

This study was supported by the Sichuan Science and Technology Support Program (2010GZ0146) as well as the Sichuan International Scientific and Technological Cooperation and Exchanges in Research Programs (2010HH0011).

REFERENCES

1. Rokkanen, P. U.; Bostman, O.; Hirvensalo, E.; Makela, E. A.; Partio, E. K.; Patiala, H.; Vainionpaa, S. I.; Vihtonen, K.; Tormala, P. *Biomaterials* **2000**, *21*, 2607.
2. Middleton, J. C.; Tipton, A. J. *Biomaterials* **2000**, *21*, 2335.
3. Gogolewski, S.; Pineda, L.; Busing, C. M. *Biomaterials* **2000**, *21*, 2513.
4. Wang, Z. Y.; Zhao, Y. M.; Wang, F.; Wang, J. *J. Appl. Polym. Sci.* **2006**, *99*, 244.
5. Russias, J.; Saiz, E.; Nalla, R. K.; Gryn, K.; Ritchie, R. O.; Tomsia, A. P. *Mater. Sci. Eng. C* **2006**, *26*, 1289.
6. Navarro, M.; Ginebra, M. P.; Planell, J. A. *Acta Biomater.* **2005**, *1*, 411.
7. Bondeson, D.; Oksman, K. *Comp. A* **2007**, *38*, 2486.
8. Yang, J.; Shi, G. X.; Bei, J. Z.; Wang, S. G.; Cao, Y. L.; Shang, Q. X.; Yang, G. H.; Wang, W. J. *J. Biomed. Mater. Res.* **2002**, *62*, 438.
9. Liu, H.; Wang, S. D.; Qi, N. *J. Appl. Polym. Sci.* **2012**, *125*, E468.
10. Mario, H.; Gutierrez, V.; Mayra, G.; Ulloa, H.; Jose, G.; Gaona, L. *J. Appl. Polym. Sci.* **2008**, *110*, 163.
11. Kallrot, M.; Edlund, U.; Albertsson, A. C. *Biomaterials* **2006**, *27*, 1788.
12. Cheruthazhekatt, S.; Cernak, M.; Slavicek, P.; Havel, J. *J. Appl. Biomed.* **2010**, *8*, 55.
13. Gursel, S. A.; Gubler, L.; Gupta, B.; Scherer, G. G. *Adv. Polym. Sci.* **2008**, *215*, 157.
14. Ghosh, P.; Siddhanta, S. K.; Chakrabarti, A. *Eur. Polym. J.* **1999**, *35*, 699.
15. Brunius, C. F.; Edlund, U.; Albertsson, A. *J. Polym. Sci. Part A: Polym. Chem.* **2002**, *40*, 3652.
16. Su, Y. C.; Kuo, S. W.; Yei, D. R.; Xu, H. Y.; Chao, F. C. *Polymer* **2003**, *44*, 2187.
17. Chen, H.; Peng, C. R.; Yao, Y. Y.; Wang, J. X.; Chen, Z. P.; Yang, Z. R.; Xia, L. J.; Liu, S. Y. *J. Appl. Polym. Sci.* **2009**, *114*, 3152.
18. Li, S. J. *Biomed. Mater. Res.* **1999**, *48*, 342.
19. Burg, K. J. L.; Shalaby, S. W. *J. Biomater. Sci. Polym. Ed.* **1998**, *9*, 15.
20. Fischer, E. W.; Hans, J. S.; Wegner, G. *Colloid. Polym. Sci.* **1973**, *251*, 980.
21. Schmitt, E. A.; Flanagan, D. R.; Linhardt, R. J. *Macromolecules* **1994**, *27*, 743.
22. Li, S.; McCarthy, S. *Biomaterials* **1999**, *20*, 35.
23. Benson, R. S. *Nucl. Instrum. Methods Phys. Res.* **2002**, *191*, 752.
24. VonRecum, H. A.; Cleek, R. L.; Eskin, S. G.; Mikos, A. G. *Biomaterials* **1995**, *16*, 441.
25. Bogatyrev, V. M.; Borisenko, N. V.; Pokrovskii, V. A. *Russ. J. Appl. Chem.* **2001**, *74*, 839.
26. Peniche, C.; Zaldivar, D.; Pazos, M.; Paz, S.; Bulay, A.; Roman. J. S. *J. Appl. Polym. Sci.* **1993**, *50*, 485.
27. Kallrot, M.; Edlund, U.; Albertsson, A. C. *Biomacromolecules* **2007**, *8*, 2492.
28. Ishii, D.; Ying, T. H.; Mahara, A.; Murakami, S.; Yamaoka, T.; Lee, W.; Iwata, T. *Biomacromolecules* **2009**, *10*, 237.